PROCEEDINGS
OF THE
NATIONAL ACADEMY OF SCIENCES

Volume 8 MAY 15, 1922 Number 5

# NOTE ON X-RAY SPECTRA

By William Duane and R. A. Patterson

Jefferson Physical Laboratory, Harvard University, and Sloane Physical Laboratory, Yale University

Communicated March 20, 1922

In previous papers[1] the authors have presented measurements of the critical absorption wave-lengths belonging to the $L$ series of nine of the heavy elements (27 wave-lengths in all). We have also discussed the bearing of these data on theoretical matters, and their relation to other available measurements of X-ray spectra. Since these papers were published, many accurate measurements have been made of the emission spectra in both the $L$ and $M$ series for the heavy elements.

Coster,[2] working in Siegbahn's laboratory, has accurately measured the $L$ series emission lines for eleven heavy elements. He has extended the three known $M$ absorption limits to five for uranium and thorium, and has measured the first three $M$ limits for bismuth.

De Broglie and Dauvillier[3] have studied in detail the $L$ series emission spectra for six heavy elements.

With these new, accurate data, Smekal,[4] Coster,[2] Dauvillier[3] and Wentzel[5] have constructed atomic systems to explain the source of each known emission line. The systems are based on the Bohr-Sommerfeld theory of the origin of characteristic X-radiation. In developing and discussing their systems, these investigators have used the values of the $L$ absorption limits measured by us. Certain criticisms have been made of a few of our values. It has therefore seemed desirable to measure some of the limits again.

Coster[6] has suggested a possible source of error in our values for the absorption limits of tungsten on the ground that we used an X-ray tube equipped with a tungsten anticathode, and that therefore we would get an effect not due to absorption alone but also to the neighboring emission lines. We wish to call attention to the fact (stated on page 534 of our paper in the *Physical Review*, Dec. 1920) that we took[7] the precaution

of using an X-ray tube with a molybdenum target to avoid exactly this difficulty. If there had been an appreciable amount of tungsten on the anticathode due to sputtering, we would have detected the presence of the strong emission lines of the $L$ series. In a more recent paper Coster[8] states that he has measured the $L_1$ and $L_2$ absorption limits of tungsten and obtained essentially the same wave-lengths as those given by us.

Table I contains our new values for the $L_2$ and $L_3$ absorption limits of Pt, Au and Bi. These measurements were taken with almost the same arrangement of apparatus as before. The X-ray tube was provided with an arm which reached nearly to the first slit of the spectrometer, thus reducing the absorption of X-rays by air. At the end of this arm and also on the front of the ionization chamber thin mica windows were employed which still further reduced the absorption of X-radiation. Finally the sensitivity of our electrometer had been increased many times. We were thus supplied with a much more sensitive detector of X-ray spectra than in our earlier measurements. This enabled us to use narrower slits and to obtain at the same time greater drops in our ionization currents for the absorption limits.

TABLE 1

CRITICAL ABSORPTION. $L$ SERIES OF X-RAYS

GRATING SPACE FOR CALCITE, $2d = (6.056 \pm 0.004) \times 10^{-8}$ CM.

| CHEMICAL ELEMENT | $L_2$ $\lambda \times 10^8$ cm. | $\nu/\nu_\infty$ | $L_3$ $\lambda \times 10^8$ cm. | $\nu/\nu_\infty$ |
|---|---|---|---|---|
| Pt | .9318 ± 3 | 0.9779 | .8918 ± 9 | 1.022 |
| Au | .9008 ± 4 | 1.0116 | .8610 ± 9 | 1.058 |
| Bi | .7871 ± 4 | 1.1578 | .7562 ± 9 | 1.205 |

In the first column for each limit is given the wave-length in Ångstrom units; in the second, the wave number divided by the Rydberg constant.

Our new value for $L_2$ of Au differs from our previous one by 0.17 per cent. The error in our previous work was due to the proximity of the bromine ionization limit, which has a wave-length $= 0.91796 \times 10^{-8}$ cm. In our new measurements it was unnecessary to have ethyl bromide in the ionization chamber.

For the $L_3$ limits to Pt and Bi the new values differ from the old ones by a considerable amount in excess of our then estimated error. These errors were undoubtedly inherent in the faintness of the effect which we were endeavoring to measure.

The other three values are substantially the same as we gave before. We do not find the error in $L_3$ for Au suggested by Dauvillier.

At the time of our previous investigation, the available evidence seemed to indicate that the $\beta_5$ and $\gamma_2$ emission lines belonged, respectively, to the $L_1$ and $L_2$ groups—i.e., that $\beta_5$ was emitted when an electron fell into the $L_1$ orbit, and $\gamma_2$ when an electron fell into the $L_2$ orbit. As we definitely proved that the $L_1$ and $L_2$ absorption limits for tungsten were of lower

frequency than $\beta_5$ and $\gamma_2$ (a fact since verified by Coster), the idea of absorption limits being "limiting frequencies" for groups of emission lines was confronted with an anomaly. We proposed an explanation of this apparent anomaly that was in accord with the Bohr theory. Since then, however, Hoyt[9] and Dauvillier[3] have pointed out that the $W$ emission line at $\lambda 1.212$ should be taken as $\beta_5$ instead of the one at $\lambda 1.203$ as before. This suggestion has been confirmed by the more accurate measurements of the corresponding line for the other heavy elements. When the square root of the frequency is plotted against atomic number for the $\beta_5$ lines, the points all lie on a smooth curve. Furthermore, in place of $\gamma_2$, the work of Dauvillier and Coster indicates that a new $\gamma$ line, $\gamma_6$, at $\lambda = 1.072$, is the result of an electron falling into the $L_2$ orbit, and therefore belongs to the $L_2$ group. Both the old $\beta_5$ line for $W$ and the $\gamma_2$ lines have been assigned to the $L_3$ group.

Consequently, we now take $\beta_5$, $\gamma_6$ and $\gamma_4$ to be the shortest emission wave-lengths in the $L_1$, $L_2$ and $L_3$ groups, respectively.

Coster has compared his new values for the wave-lengths of each of these emission lines with our values of the corresponding absorption limits, and has concluded that the absorption limits are in general somewhat shorter in wave-length than the emission lines associated with them. Table II gives this comparison using our new values for $L_2$ and $L_3$.

TABLE II

| ELEMENT | $L_2$ | $\gamma_6$ | $L_3$ | $\gamma_4$ |
|---|---|---|---|---|
| Pt | .9318 ± 3 | .9317 | .8918 ± 9 | .8950 |
| Au | .9008 ± 4 | .90125 | .8610 ± 9 | .8663 |
| Bi | .7871 ± 4 | .7874 | .7562 ± 9 | .7610 |

Within experimental error the wave-lengths of the absorption limits are shorter than the wave-lengths of the shortest emission lines associated with them.

Coster[2] now places the number of $L$ doublets at four, $\eta - l$, $\beta_2 - \alpha_2$, $\gamma_5 - \beta_6$, $\gamma_6 - \beta_5$. The $\gamma_1 - \beta_2$ doublet has been eliminated which is in accord with our suggestion that the electrons responsible for these two lines do not appear to start from the same orbit but different ones. He has also found and measured the two $M$ absorption limits predicted by us for U and Th in order to explain the existence of the $\eta - l$ doublet. His values are in close agreement with our predicted ones.

According to Smekal,[4] the $M\gamma$ line is due to the passage of an electron from an $N_3$ orbit to an $M_3$ orbit. If this is true, the following relation between frequencies should hold:

$$(L_3 - L_1) - M\gamma = L\beta_3 - L\beta_2$$

Coster has tested this relation using his new values for $\beta_2$ and $\beta_3$, Stenstrom's value for $M\gamma$ and our values of $L_1$ and $L_3$. He finds it confirmed by the available experimental data except in the cases of Pt and Bi. Our

new values bring Pt into line. For Bi, however, our correction is in the right sense but far too large. We cannot at present explain this discrepancy. Table III gives our new values for this relation.

TABLE III

| ELEMENT | $L_2 - L_1$ | $M\gamma$ | $(L_3 - L_1) - M$ | $\beta_3 - \beta$ |
|---|---|---|---|---|
| Pt | .1706 | .17158 | —.0010 | .0000 |
| Bi | .2163 | .20144 | +.0149 | +.0176 |

The lines $\beta_7$ and $\gamma_4$ have been assigned by Coster to electrons which start from *different* outer orbits and fall, respectively, into $L_1$ and $L_3$ orbits. Assuming the $\gamma_4$ electron to start from a higher orbit than $\beta_7$, we should then expect $\gamma_4 - (L_3 - L_1)$ to be greater than $\beta_7$. Coster shows this to be the case except for Pt and Bi. Our new measurements bring both Pt and Bi into line with the other elements. Table IV contains values for these quantities in the cases of Pt and Bi.

TABLE IV

| ELEMENT | $\lambda_4 - (L_3 - L_1)$ | $\beta_7$ | $\Delta$ |
|---|---|---|---|
| Pt | 847.8 | 844.9 | +2.9 |
| Bi | 980.6 | (977.2) | +3.4 |

The value of $\beta_7$ for Bi was obtained, as suggested by Coster, by interpolation based upon the constant difference in wave-length exhibited by the elements for $\beta_2 - \beta_7$, the wave-length for $\beta_2$ being known. The differences in the fourth column are in the same sense and of the same magnitude as those found by Coster for Ta, W, Au, Tl and Pb. Moreover, if we estimate a value for the wave-length of $\gamma_4$ for U based upon our value of $L_3$ for the same element, we obtain a difference greater than those above and also in the same sense. It is therefore quite well established that the $\beta_7$ and $\gamma_4$ electrons start from orbits which maintain approximately the same difference in energy level as we go from Ta to U.

The authors in 1920 compared the frequencies of certain $L$ emission lines with the differences in frequency between corresponding $L$ and $M$ absorption limits.[1] Kossel first pointed out that these quantities should be equal on Bohr's theory. At that time we found each $L$ emission frequency to be equal to a corresponding difference in absorption frequencies within the limits of experimental error. Coster[2,3] has recently extended this comparison with his new and more accurate measurements to in-

TABLE V

| ELEMENT | $\beta$ | $L_1 - M_5$ | $\eta$ | $L_2 - M_5$ | $\alpha_1$ | $L_3 - M_1$ | $\alpha_2$ | $L_3 - M_2$ |
|---|---|---|---|---|---|---|---|---|
| U | 855.84 | 855.1 | 1134.95 | 1131.8 | 1003.23 | 1002.17 | 990.37 | 989.21 |
| Th | 819.19 | 818.8 | —— | —— | 955.78 | 954.80 | 944.08 | 943.15 |
| Bi | —— | —— | —— | —— | 798.54 | 797.43 | 790.20 | 789.35 |
| | $\beta_1$ | $L_2 - M_2$ | $\beta_3$ | $L_3 - N_3$ | $\beta_4$ | $L_3 - M_4$ | | |
| U | 1269.08 | 1265.87 | 1286.29 | 1285.78 | 1222.53 | 1220.86 | | |
| Th | 1194.94 | 1193.15 | 1211.67 | 1209.77 | 1155.00 | 1151.86 | | |
| Bi | 959.93 | 958.16 | 973.85 | 971.2 | —— | —— | | |

clude two more $M$ absorption frequencies for U and Th, and the first three $M$ limits for Bi. Table V contains his values with the exception of $L_3 - M_3$ for Bi which we have corrected to accord with our new value of $L_3$ for that element.

In each case the emission frequency exceeds the difference in absorption frequencies, but by an amount that is less than 0.3 of a per cent.

*The K Series of Molybdenum.*—The authors have also measured the emission and absorption spectra for the $K$ series of molybdenum. The apparatus and method used are described in previous papers.[7] A Coolidge tube equipped with a molybdenum target and an extra arm at the end of which happened to be a thin glass window served as the source of radiation.

Table VI contains the results of these measurements.

TABLE VI

K SERIES OF MOLYBDENUM

GRATING SPACE OF CALCITE = $2d$ = 6.056 $(10)^{-8}$ CM.

| LINE | NO. | GLANCING ANGLE | WAVE-LENGTH × $(10)^8$ CM. | ORDER |
|---|---|---|---|---|
| $\alpha_2$ | 3 | 13°–36′–08″ | 0.71213 ± 8 | 2d |
| $\alpha_1$ | 3 | 13°–31′–07″ | 0.70783 ± 7 | 2d |
| $\beta'$ | 3 | 12°–02′–50″ | 0.6320 ± 2 | 2d |
| $\beta$ | 6 | 12°–01′–50″ | 0.63114 ± 7 | 2d |
| $\beta\beta'$ | 1 | 5°–59′–05″ | 0.6314 ± 3 | 1st |
| $\gamma$ | 3 | 11°–48′–32″ | 0.6197 ± 2 | 2d |
| $\gamma$ | 1 | 5°–52′–30″ | 0.6199 ± 3 | 1st |
| $K$ | 1 | 5°–51′–40″ | 0.6184 ± 2 | 1st |

In the second column the number is the number of actual measurements made.

In the second order, the $\beta$ line was markedly asymmetrical and we were able to estimate the position of its weaker component, $\beta'$, predicted by Sommerfeld. The wave-length difference between these two lines is of the same order of magnitude as that found in the case of other elements. The wave-lengths of $\beta$ and $\gamma$ found in the first order are definitely longer than those found in the second order. This is chiefly due to the complex structure of both of these lines, although several investigators including the authors have found a similar but smaller effect in the case of emission lines supposed to be single.

In a recent paper Overn[10] has also given wave-lengths for these same emission lines. His values, however, do not agree with ours even when corrected for the difference between the rock salt grating space used by him and the calcite grating space used by us. The discrepancy between his values and ours seems to increase as we go farther from the "white line" used as a reference line by him.

As we determined these wave-lengths by the ionization method, we are also able to give the ratio of the intensities of $\alpha_1$ and $\alpha_2$. From three de-

terminations in the second order we obtain for this ratio 1.97 as compared with 2.00 predicted by Bohr.

The ratio of the intensities of $\beta$ to $\gamma$ in the first order is 6.3 (one determination) and in the second order is 5.46 (two determinations).

[1] Duane and Patterson, *Proc. Nat. Acad. Sci., Washington*, Sept. 1920; *Phys. Rev.*, Dec. 1920, p. 526.

[2] Coster, *Z. Phys.*, **5**, 1921 (139); also **6**, 1921 (185).

[3] De Broglie and Dauvillier, *Paris, C. R.*, **173**, p. 137. Dauvillier, *Ibid.*, **172**, also **173**, p. 647, also other papers in this volume.

[4] Smekal, *Z. Phys.*, **5**, 1921 (91, 121). Also **4**, 1921.

[5] Wentzel, *Ibid.*, **6**, 1921 (2).

[6] Coster, *Ibid.*, **5**, 1921 (147). Also *Physic Rev.*, Sept. 1921.

[7] Duane and Patterson, *Physic Rev.*, **16**, 1920 (534).

[8] Coster, *Ibid.*, Jan. 1922.

[9] Hoyt, *Proc. Nat. Acad. Sci., Washington*, Nov. 1920.

[10] Overn, *Physic. Rev.*, Nov. 1921, p. 350.

---

## *A NEW METHOD OF USING X-RAYS IN CRYSTAL ANALYSIS*

By George L. Clark and William Duane

Jefferson Physical Laboratory, Harvard University

Communicated April 4, 1922

The procedure described in this paper differs in some fundamental details from the elegant methods of analyzing crystals by means of X-rays developed by Laue, the Braggs and others.

The substance to be examined may be in the form of powder or of whole crystals. In the latter case the crystal need not be large. One having a volume of only .25 cubic mm. suffices, although slightly more accurate data may be obtained, if it has a somewhat larger volume.

In our method we employ X-rays belonging to the continuous spectrum, and therefore containing rays of a great variety of wave-lengths, and not the line spectra of definite wave-lengths, as in most other methods. This procedure has certain advantages. An ordinary X-ray tube with a tungsten target may be used, and high voltages may be applied to it. More intense X-radiation can be obtained from tungsten than from such chemical elements as rhodium and molybdenum. Further in some cases it is desirable to employ X-rays of shorter wave-lengths than those in the $K$ series of rhodium and molybdenum, for these shorter rays are more penetrating than the longer ones. As a rule we use the spectrum between .12 and .80 Ångström.

In making an analysis of a small crystal we place it at the center of an X-ray spectrometer, provided with an ionization chamber and a quadrant electrometer. The slits of the instrument should be fairly narrow, and

the best results can be obtained by turning the X-ray tube so that the rays that pass through the instrument leave the target almost grazing its surface. This gives a narrow beam of rays. We set the ionization chamber so that the line from the axis of rotation to the chamber's slit makes an angle, $2\theta$, of convenient size (usually about 10°) with the direct beam of rays. Keeping the ionization chamber always in the same position we turn the crystal around by successive small steps and measure the ionization current at each step. When a set of parallel planes in the crystal lie at an angle $\theta$ to the incident beam of rays the planes pick out of the beam X-rays of certain definite wave-lengths, $\lambda$, and reflect them into the chamber, and we get a marked increase in the ionization current. Evidently the angles between the positions of the crystal that correspond to maximum ionization currents are the angles between the crystal planes.

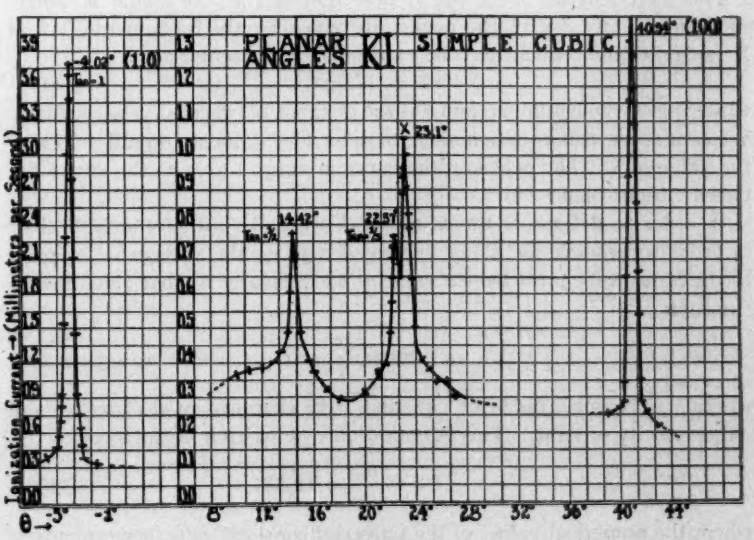


FIGURE 1

The curve in figure 1 represents the ionization current as a function of the position of the crystal in an experiment with potassium iodide. The salt came from Professor Baxter's laboratory, and was of exceptional purity. The peaks on the curve are sharply marked, and their angular positions can be estimated to within less than 0°.01. The angles between several pairs of peaks are 44°.96, 18°.37 and 26°.52, which correspond very closely with the angles between some of the principal planes in a cubic lattice, namely, 45°, 18°.43 and 26°.57. This together with a similar ex-

periment performed with the crystal turned through 90° indicates that *KI* has a cubic lattice, which agrees with previous work by Davey and Wyckoff. The accuracy with which the experimentally determined angles agree with those given by solid geometry amounts in reality to a test of the precision with which the instrument has been set up, i.e., so that an axis of the crystal lies parallel to the axis of rotation, and so that the center of the incident beam of rays and the effective reflecting plane of the crystal lie on the axis of rotation.

One peak of the curve, marked $X$, does not correspond to any of the chief planes of the crystal, i.e., those with small indices. Its position shows that the corresponding planes make an angle of 17°.84 with the 100 planes. Possibly the marked reflection at this angle may be due to the characteristic line spectrum of iodine. Further evidence on this point will be given in a later paragraph.

The wave-lengths, $\lambda$, of the X-rays reflected at the angle $\theta$, corresponding to any one of the peaks, are given by the fundamental law of X-ray reflection, which may be expressed by the equation

$$n\lambda = 2d \sin \theta, \qquad (1)$$

where $n$ is a whole number, and $d$ is the distance between successive planes. We cannot use this equation alone to determine $d$, for we do not yet know the value of $\lambda$. The peaks on the curve in figure 1 give us the angles between various planes only.

In order to determine the distance, $d$, we make use of the fact[1] that, in order to produce an X-ray of wave-length $\gamma$, the voltage, $V$, applied to the X-ray tube must have a value at least as large as that given by the equation

$$Ve = \frac{hc}{\lambda}, \qquad (2)$$

where $h$ is Planck's radiation constant, $e$ the charge of an electron (e) and $c$ the velocity of light. This equation may be written in the form

$$V\lambda = \frac{hc}{e} = 12{,}354, \qquad (2')$$

where the numerical value[2] of the universal constant, $hc/e$, corresponds to $V$ expressed in volts and $\gamma$ in Ångströms.

In an actual experiment to measure $d$ we set the crystal so that the X-rays reflected by the planes we desire to investigate enter the ionization chamber (i.e., we set on one of the peaks in the curve of figure 1), and reduce the voltage until the ionization current sensibly vanishes. The voltage at which it vanishes is sharply marked, especially if the voltage is a constant one, from a storage battery, for instance. It is a good plan to increase the current through the tube at the same time as the voltage decreases in such a way as to keep the product of the two, that is, the

power delivered to the tube, constant. Evidently the ionization current will not completely vanish until the voltage becomes so low that it cannot produce the *longest* X-rays reflected at the angle $\theta$ according to equation (1). The longest waves correspond to $n = 1$.

A small correction has to be added to the angle $\theta$ due to the fact that the source of rays and the slit of the spectrometer have finite breadths. The rays in the incident beam are not all exactly parallel to each other and the correction equals half the angle between the rays that deviate most from the central ray on its two sides. This angle is the breadth of the source plus the breadth of the slit divided by the distance between them. The correction is usually small. In our experiments it amounts to about 3′ of arc, which is less than one per cent of the corrected value of $\theta = 5°.51$ used in the first illustrative case described below.

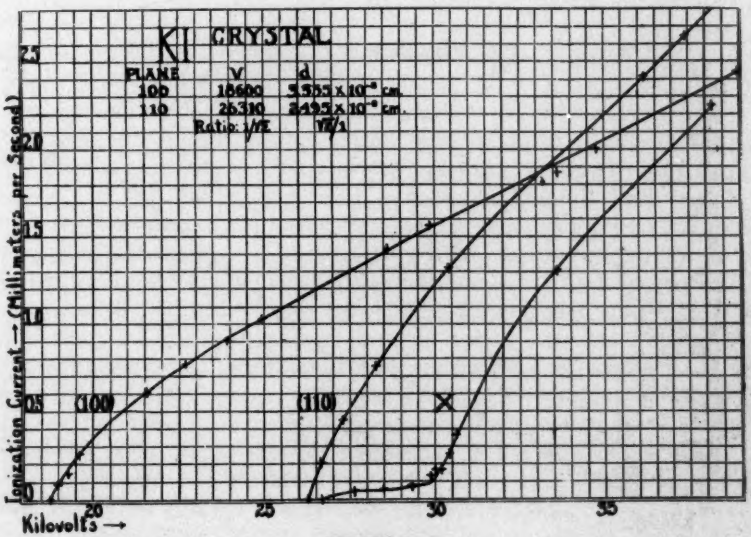


FIGURE 2

The curves in figure 2 represent the ionization currents as functions of the voltages for three of the peaks of figure 1. The voltages at which the ionization currents vanish for the peaks marked 100 and 110, respectively, are 18,600 and 26,310 volts.

Eliminating $\lambda$ between equations (1) and (2′) we get, with $n = 1$,

$$d = \frac{12{,}354}{2V\sin\theta}. \qquad (3)$$

Substituting in this $\theta = 5°.51$ and the values of $V$, we find for $d$ the 3.535 and 2.495 Ångströms, respectively. The ratio of the first to the

second is 1.417, which differs little from $\sqrt{2} = 1.414$, the value it should have in a cubic crystal. Taking 3.532 as the average length of the edge of a cube, and assuming one atom to each cube the calculated density of *KI* comes out 3.111, in close agreement with the density 3.114 measured by Baxter.

Equation (3) contains a universal constant $\frac{hc}{e} = 12{,}354$ and two quantities, a voltage, $V$, and an angle, $\theta$, both of which we measure. The values of $d$, therefore, determined by this method are independent of previous measurements of the distance between the planes in any crystal. This advantage is, perhaps, more theoretical than practical at present, for measurements with X-rays reflected from calcite probably furnish us the most accurate estimates we have for the universal constant.

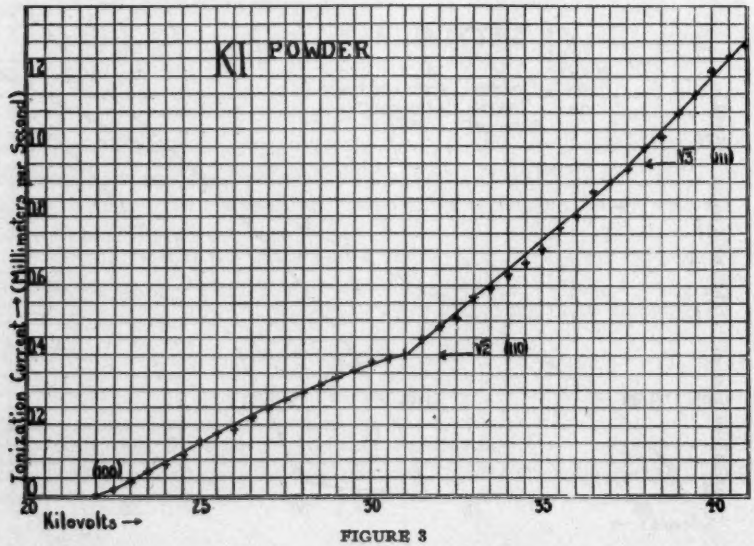


FIGURE 3

The agreement between the distances, $d$, determined by this method with those calculated from the density, atomic weights, etc., helps to confirm the general correctness of the laws of X-rays as at present understood.

If the specimen to be examined has the form of powder, we place the powder at the center of the spectrometer, fix the position of the ionization chamber at an angle $2\theta$ and reduce the voltage by steps making measurements of the ionization current as before. The ionization current vanishes when the voltage is no longer able to produce the longest X-rays that are reflected at the angle $\theta$ by the powder. This maximum wave-length corresponds to $n = 1$ in equation (1) and to the greatest distance $d$ be-

tween successive planes in the crystal that are alike. The curve in figure 3 represents the ionization current as a function of the voltage in an experiment with potassium iodide powder. In addition to the point where the ionization current vanishes there are several well-marked places where the curvature changes abruptly. The voltages at these breaks in the curve are the voltages at which the rays reflected from other crystal planes cease to be produced. These voltages together with the angle $\theta$, substituted in equation (3), give the corresponding distances between the planes. The three most sharply determined voltages are 21,740, 31,010 and 37,600 volts, respectively. The ratios of these numbers to each other differ from $\sqrt{2}$ and $\sqrt{3}$ by small fractions of one per cent only. They correspond, therefore, to the 100, 110 and 111 planes, respectively, of a cubic lattice. The angle $\theta$ equals 4°.51 in this experiment, and the average value of $d$, calculated from equation (3), is 3.534, in close agreement with that obtained in the above-described measurement with a small crystal of potassium iodide.

The curve marked $X$ in figure 2 corresponds to the peak marked $X$ in figure 1. There appears to be a sharply indicated point of inflection in the former at a voltage of 30,000 volts. Substituting this in equation (2′) we find that the corresponding wave-length is .412. This wave-length is a good mean value of the wave-lengths of $\alpha$ and $\beta$ lines in the $K$ series of iodine, namely, .437 and .388. 30,000 volts do not suffice to produce the $K$ series of iodine. If, however, one sets a spectrometer on a characteristic line and reduces the voltage, the ionization current does not vanish when the voltage ceases to produce the characteristic X-rays. It vanishes only when the voltage becomes insufficient to produce an X-ray in the continuous spectrum of equal wave-length to that of the characteristic line. We have tested the existence of the peak $X$ by turning the crystal as in the experiments represented in figure 1 with voltages in the neighborhood of 33,030 volts, which is the critical voltage for the production of the $K$ series of iodine. We find no evidence of a peak at a voltage slightly below 33,000. The peak is just observable, however, if the voltage equals 33,500 volts. These points strongly favor the idea that the characteristic $K$ radiation of iodine produces the peak $X$. The distance between the planes making an angle of 17°.84 with the 100 planes, however, does not equal that calculated from equations (1) and (3). The former is 1.088 and the latter is 2.144, i.e., about twice the former. Perhaps this may be due to the fact that only half the atoms are iodine. If the characteristic radiation does produce the peak, and, if we adopt the interference of scattered rays as the explanation of X-ray reflection, we must assume that, on the average at least, definite time relations must exist between the passage of the primary X-ray across an atom and the emission of a secondary *characteristic* ray. If we adopt the quantum point

of view, we must suppose that the direction in which the characteristic ray travels depends upon neighboring atoms as well as upon the angle of incidence of the primary beam.

The relative reflecting power of different planes may be determined by reflecting from them the *same* portion of the continuous spectrum, or different portions having known relative intensities. The use of the continuous spectrum for this purpose instead of the line spectrum has the advantage of flexibility. One can employ short, penetrating X-rays, and with these investigate dense crystals of high absorbing power.

[1] *Phys. Rev., Ithaca*, Aug. 1915, p. 166.
[2] *J. Optical Soc.*, May 1921, p. 386.

---

## *ACOUSTIC TOPOGRAPHY VARYING WITH THE POSITION OF THE ORGAN PIPE**

By Carl Barus

Department of Physics, Brown University

Communicated March 20, 1922

1. *Introductory.*—The coördinate axes have the $x$-$y$ plane on the large table, the origin near one corner. The survey is made between walls at $y = 174$ cm. and $y = -130$ cm.; and the pipe is displaced both in the $y$ and $z$ (upward) direction. In the graphs, the letters $P$, $R$, $T$, $T'$, used either as subscripts or directly, will refer to the pipe, the resonator, the edges of the table. Throughout $s$ is the fringe deflection of the U-tube interferometer, proportional to the acoustic pressure or to the nodal density evoked at a given place ($x = 0$, $y$, $z$), by the sounding pipe $P$.

The latter was a closed brass $f''$ pipe, blown by the pipe blower elsewhere described, rigidly attached. In graphs 1–3, this is sketched in under $P$ and an arrow shows the direction of the wind current. The closed cylindrical pinhole resonator $R$, lying with its axis parallel to $y$, in the $yx$ plane (table) and moving end-on along $y$, is also suggestively indicated, showing the resonator azimuth for which the usually paired graphs apply. In the earlier work (figures 1–3) the *middle* of the resonator was used for the location of points in $y$. An inversion of the resonator thus gave the two curves for each case and they were obtained consecutively. If the mouth of $R$ is used to determine the coördinate $y$ as in figures 4, 6 to 10, but a single curve is obtained, for all azimuths of $R$. The same is true for a resonator placed with its mouth at the mean $y_R$ of a given ordinate, $s$, in case of figures 1–3.

2. *Pipe Elevated above the Origin on the Table.*—In figures 1–4 the organ pipe, with its mouth vertically above the origin, was raised succes-

sively in steps of 20 cm. from $z = 20$ cm. to $z = 80$. For each pipe level the distribution of nodal intensity along the $y$ axis was explored by moving $R$ along it (with observations taken every $\Delta y_R = 10$ cm. apart). In figure 1, $z_p = 20$ cm., there is probably some distortion at the origin, owing to the wind from the near pipe, otherwise the first crest would be in negative $y$. From the glancing incidences, this graph has less detail than figure 2 ($z_p = 40$ cm.), which preserves the same general character but is lower in $s$ and shrunk in the $y$ direction. In figure 3, $z_p = 60$ cm., the topography is totally changed. There is now a trough

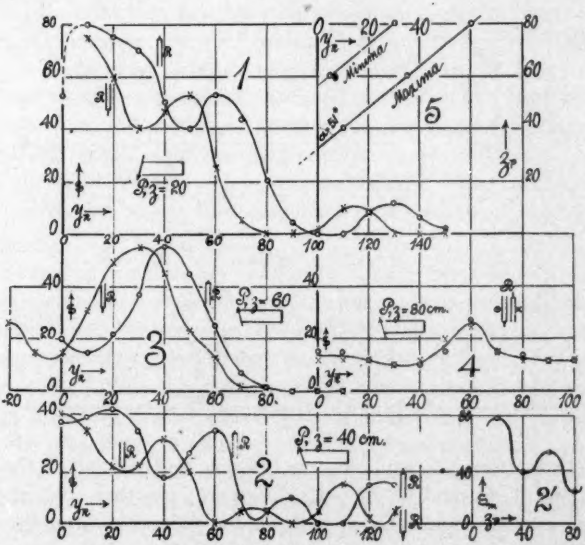


near the origin and (on compounding) but one marked crest. Figure 4, $z_p = 80$ cm., is redeveloping a crest at the origin, but otherwise preserves the former outlines. In this figure and the following, the mouth of the resonator was used to define $y_R$ so that the two curves are practically coincident.

If the highest crests correspond to like path differences and therefore belong together, their position $y_R$, $z_p$ in figure 5 is seen to progress roughly along a straight line $y = 1.25z - 40$, the slope $dy/dz$ corresponding to an angle of incidence of $\alpha = 51°$. The minima determine parallel lines, the vertical distance apart of consecutive lines being here $\Delta z_p = 24$ cm. or about half a wave-length.

Furthermore, the graphs, as a whole, are alternately high and low in intensity, $s$. If the intensity $s_m$ of the highest crest be expressed in terms of the pipe elevation $z_p$, the resulting graph, figure 2′ (scale $^1/_2$), presents

the same strongly marked harmonic character of the reflection graphs of the preceding paper. Cf. § 3.

3. *Pipe Displaced in a Given Level along y.*—Figures 6–10 are constructed on the same plan as the preceding, the ordinates $s$, denoting fringe deflections or the nodal intensity, encountered by the mouth of the resonator at $y_R$. If the ordinates be also taken as $z_p$, the pipe position, $P$, etc., may also be indicated on the graphs. $T$, $T'$ show the edges of the table. In figure 6, where the pipe is 40 cm. above the origin, the graph is highly detailed with crests mostly 30 cm. apart. The hyperbolas

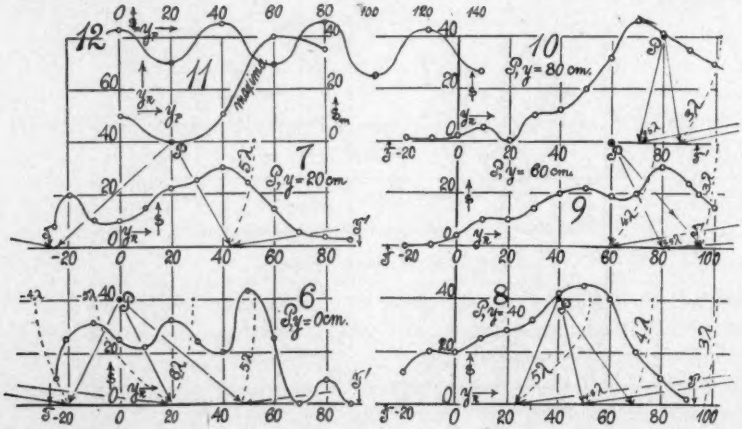


for reflections from the wall at $y = 174$ cm. and beyond $T'$ have been sketched in at $5\lambda$ and $6\lambda$ of path difference, together with the corresponding acoustic rays. So also those for reflection from the wall at $y = -130$ cm. (beyond $T$). The last agrees badly with the crest observed at about $-10$ cm. The alluring possibility of an intersection of the positive and negative hyperbolas resulting in very high crests does not work out. In figure 7 also the positive hyperbola $5\lambda$ fairly corresponds to the observed crest, but not the negative one. In figures 8, 9, 10 the positive hyperbolas $3\lambda$, $4\lambda$, $5\lambda$, also, fail of coincidence with the observed crests. These in fact lie nearly between them, or half a wave-length of path difference beyond. Thus it seems improbable that the maxima and minima can be explained as resulting from the reflection at these walls, while all other walls and the ceiling are far more distant.

In figures 6–10 one is often in doubt as to which of the crests belong together. Crests seem rather to separate and recombine. Taking the highest in the successive curves, figure 11 shows that the relation of pipe and resonator positions for maxima is here not simple as in figure 5. In fact the pipe approaches the high crest and finally overtakes it (figure 10).

There is no symmetry of graph at the middle of the table ($y = 33$) and the two edges $T$, $T'$ show no correspondence. The graphs may actually be traced into free air beyond the table, as indicated in the prolongation of figure 12. Finally if the intensity $s_m$ of the supposedly chief maxima be laid off in terms of the pipe position an harmonic figure 12 of relatively constant amplitude appears in reasonable contrast with the curve of diminishing amplitude in figure 2′, for the raised pipe. In both cases, the steps of 20 cm. between pipe positions are too large for sharp discriminations; but it is noticeable that the distance between crests in figures 2′, 12 and the earlier reflection figures is about $\Delta y = 40$ cm. The prevailing $\Delta y$ in the single graphs 2, 6, etc., is about 30 cm. In figure 12 the points beyond $y_p = 80$ cm. were obtained in similar investigations, here omitted.

4. *Summary.*—The above work as a whole has shown that when the reflecting plate is relatively near, to the pipe and resonator, the position of maxima and minima may be predicted as a case of ordinary interference and the wave-length computed satisfactorily. The distribution of intensity among the crests and troughs remains harmonic and has not been foreseen.

If the reflecting surfaces are relatively remote the positions of crests and troughs cannot, as a rule, be found by the same method satisfactorily. In certain instances, there seemed to be an approximate fit; but as a whole the attempt was unsuccessful and the distribution of nodal intensities equally puzzling. Acoustic topography is not symmetrical to the pipe. It appeared, however, that, when the organ pipe, definitely placed, is sounded, the occurrence of nodal surfaces of a fixed position in free air is demonstrable everywhere. Distributions between walls are consistent and differ from distributions between wall and door. It is not improbable, moreover, that such surfaces are regularly grouped and may for reasonable distances be approximately parallel. If then they are intersected obliquely, for instance by the plane of the table, and if $\alpha$ is the mean angle between the latter and the nodal surface, the distance between crests on the table should be $\Delta y = \lambda/(2 \sin \alpha)$. Hence this intercept, $\Delta y$, may have any value depending upon the general shape of the room. If the prevailing value $\Delta y = 30$ cm. be taken, $\sin \alpha = 24/30$ or $\alpha = 53°$ roughly. This angle between surfaces is also the angle of incidence of the rays, and has been encountered more or less closely in other instances (fig. 5). The distribution of intensities would then also depend on the fixed pipe position in relation to the given room, regarded integrally as an enveloping reflector. Such an explanation is plausible and flexible, no doubt; but it has the great disadvantage that none of the results can be reproduced by computation. The conviction that some other explanation may be found is not removed and the answer probably lurks in such curves as figures 2′ and 12. This is particularly so, because the pin-

hole resonator is practically unresponsive to antinodes and to wave trains except within ranges from the pipe which are small as compared with the dimensions of the room as a whole.

* Advance note from a Report to the Carnegie Institution of Washington, D. C.

---

## ON STEERING AN AUTOMOBILE AROUND A CORNER

By A. G. Webster

Department of Physics, Clark University

Read before the Academy April 25, 1921; received April 6, 1922

The question of so arranging the steering gear of an automobile that the front wheels shall skid as little as possible owing to axes not intersecting has been dealt with by A. L. Candy (*American Mathematical Monthly*, June 1920) and leads to a geometrical discussion of a high degree of complexity. The present somewhat trifling paper has no such ambitious purpose, but was suggested by a question asked on the witness-stand as to how much an automobile must turn out in order to pass another. It was necessary to make some assumption, and this led to the question of steering in general, and the principles that should govern it. We shall consider only the question of passing from a straight course to another at right angles therewith at constant velocity, and inquire how we must steer in order not to skid.

The layman ignorant of geometry and dynamics will suppose that we describe a circle, but this is impossible, not only because it is impossible to put the helm over suddenly so as to change from zero to a finite curvature, but also because the sudden change in the centrifugal force from zero to a finite quantity would produce a wholly intolerable shock. Inasmuch as the question of transition railroad curves has received so much attention, it is thought that the treatment of this question for an automobile may have some interest to engineers. We shall for the present neglect the fact that the rear wheels do not track with the forward ones, taking that up later as a correction. Thus we shall examine the curve described by a machine of zero wheel-base, like a wheelbarrow, measuring wheel or monocycle. The condition is evidently that the curvature shall begin at zero, increase to a maximum until the tangent has turned through an angle of 45 degrees, and then return by a symmetical process.

The centrifugal force is equal to $mv^2/\rho$, where $m$ is the mass, $\rho$ the radius of curvature, $v$ the velocity, and if there is to be no skidding this must be less than $mg\mu$ where $\mu$ is the coefficient of friction, consequently we must have at all times

$$v^2/\rho < \mu g.$$

This does not, however, determine the shape of the curve, to obtain which some assumption must be made. If we assume that the mean value of the centrifugal force or, what is the same thing, of the curvature (since $v$ is constant) is to be a minimum we shall get no result, except a straight line, which would be a discontinuous solution, and inadmissible. We shall therefore assume that the mean square of the curvature is a minimum, that is

$$\delta \int \kappa^2 ds = \delta \int (d\theta/ds)^2 ds = 0,$$

subject to the condition

$$\int dx = \int \cos\theta ds = \text{constant, the length of chord.}$$

But this gives

$$d^2\theta/ds^2 + \lambda \sin\theta = 0,$$

where $\lambda$ is some constant. But this is the equation of the elastica or curve assumed by a bent flexible rod, ruler, or spline. In fact, in order to obtain the equation of the elastica, we have to make the potential energy of bending a minimum, and as this, at each point, is proportional to the square of the curvature, the problem is mathematically the same.

If we take the chord for the X-axis, we shall find the equation satisfied if we take the curvature proportional to $y$, and introducing the elliptic functions of Jacobi, with $c$ a constant of homogeneity,

$$dx/ds = \cos\theta, \quad dy/ds = \sin\theta,$$

$$\kappa = d\theta/ds = -y/c^2, d\kappa/ds = d^2\theta/ds^2 = -1/c^2 dy/ds = -1/c^2 \sin\theta,$$

$$y = a\mathrm{cn}s/c = a\mathrm{cn}u, \; dy/ds = -a/c\,\mathrm{sn}u\mathrm{dn}u = -2k\mathrm{sn}u\mathrm{dn}u,$$

where

$$s/c = u, \quad a/c = 2k,$$

from which

$$dx/ds = \sqrt{1 - 4k^2\mathrm{sn}^2u\mathrm{dn}^2u} = 2\mathrm{dn}^2u - 1,$$

$$x = 2c\int_0^{s/c} \mathrm{dn}^2u du - c\int_0^{s/c} du = c[2E(u) - u] = c[2E(k,\varphi) - F(k,\varphi)],$$

where $F$ and $E$ are Legendre's elliptic integrals of the first and second kind, respectively. The value of $k$ is determined by the fact that at the point of inflexion, where $\theta = -45°$, we have $u = \overline{K}$, the complete elliptic integral, and since $\mathrm{sn}\overline{K} = 1$ and $\mathrm{dn}\overline{K} = \sqrt{1-k_2}$ we have $2k\sqrt{1-k_2} = \sin 45°$. Putting $k = \sin\alpha$ we see that $\alpha = 22°.5$. With this value for $\alpha$ taking values of $\varphi$ at intervals of 10° from 0° to 90°, values of $x$ and $y$ are calculated by means of Legendre's table and the curve drawn, which is shown on the inside of figure 1. It fits very accurately a spline made of celluloid, held fast at the vertex, and merely by contact at the point of inflexion. We find the ratio of the maximum ordinate to the whole chord or base is .2757 and that the radius of maximum curvature is the chord divided by 2.1429.

The question now arises, how nearly does the curve actually described correspond with the above description? We may take as the simplest assumption that when the driver gets ready to turn he puts the steering wheel over with a constant velocity until he is half-way around, and then

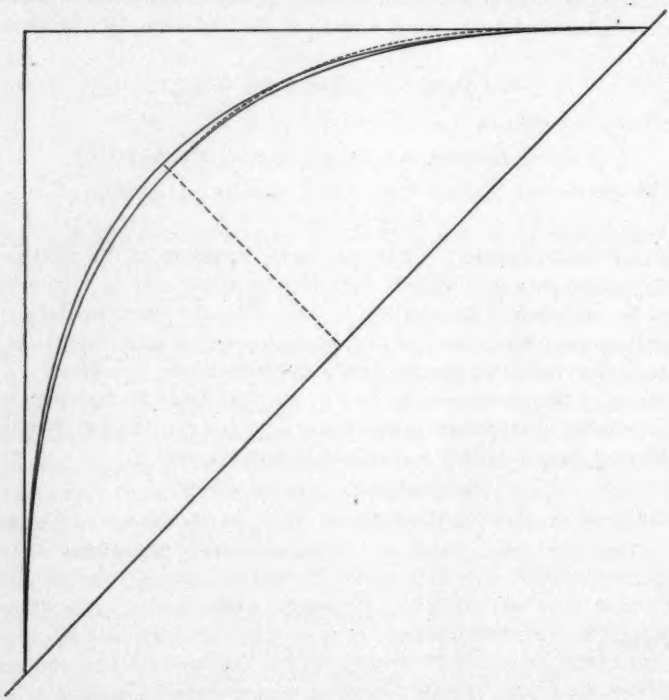

FIG. 1

turns it back with the same velocity. This is to be sure not exactly true, but as the wheel is dominated rather by friction than by inertia it will do for an approximation, and is besides about what observation shows. If the effect of this is to make the curvature of the path proportional to the time or to the distance travelled since turning (which will be shown below to be nearly the case), we have

$$\kappa = d\theta/ds = as$$

as the differential equation of the curve, where $a$ is a constant. But a curve whose curvature is proportional to the length of the arc is the well-known spiral of Cornu, used in the theory of diffraction in optics. The curve may be constructed graphically from the differential equation, but more accurately by the use of tables of Fresnel's integrals. If we put

$$x = \int_0^v \cos\pi/_2 v^2 dv, \quad y = \int_0^v \sin\pi/_2 v^2 dv,$$

we have

$$dx = \cos\pi/_2 v^2 dv, \quad dy = \sin\pi/_2 v^2 dv, \quad ds^2 = dx^2 + dy^2 = dv^2,$$
$$dy/dx = \tan\theta = \tan\pi/_2 v^2, \quad \theta = \pi/_2 v^2 = \pi/_2 s^2 = as^2/2.$$

The integrals above have been tabulated by Gilbert, and are reproduced in Verdet's *Traité d'Optique Physique*. From them the spiral has been plotted, and is shown in the outer curve in figure 1. It will be seen that it differs very little from the elastica. As a matter of fact the ratio of the maximum ordinate at right angles to the chord is .2861 compared with .2757 for the elastica. For the circle this ratio would be only .2071. The reason for the near agreement of the two curves, in one of which the curvature is proportional to the arc, and in the other to the ordinate, is of course the fact that for a considerable distance the curve is nearly straight.

The simplest assumption that could have been made for a rough calculation would have been that of a parabola, $y = ax^2$, but the ordinary parabola of order two would not do since its curvature does not vanish at the origin, and diminishes as we leave the origin. A cubical parabola would be the most obvious, but we shall do better by putting $y = ax^n$ and determining the exponent $n$ so that the curve shall pass through the vertex of the elastica and be tangent to it. We find $n = 3.458$. The curve is drawn dotted on figure 1, and lies between the other two curves. The ratio of the extreme distance from the chord to the length of the chord in the case $n = 3$ would have been .25. We consequently see that any of the four curves, the elastica, spiral of Cornu, parabola of order 3.458, or cubical parabola, will give a very good approximation to the actual path.

We have now to consider the effect of the finite length of the wheelbase, and this leads us to consider the question of steering in general. We shall first suppose for generality that both the front and rear wheels can be steered, as in a hook and ladder truck, but we shall still neglect the effect of the finite width of the track. The case contemplated is exactly realized in the bicycle. In figure 2, let $l$ be the length of the wheelbase, let $s$, $\theta$, $\alpha$, $\rho$ be the distance run, the angle made by the tangent with a fixed direction, the angle through which the wheel has been turned (that is, the angle made by the tangent to the path with the chassis, and the radius of curvature of the path, respectively, for the front wheel, and let the same letters with accents denote the corresponding quantities for the rear wheel. (When we come to consider the dynamics of the matter we shall need corresponding quantities for the center of mass, and shall denote them by two accents.) Then since the whole machine turns about the instantaneous center which is the intersection of the axes of the two

wheels, we see on reference to figure 2, $\psi$ being the angle made by the chassis with the fixed direction,

$$\rho d\theta = ds, \quad \rho' d\theta' = ds', \quad \theta + \alpha = \theta' + \alpha' = \psi.$$

We also have

$$\cos\alpha/\rho = \cos\alpha'/\rho' = \sin(\alpha - \alpha')/l,$$

which equations give $\rho$ and $\rho'$ as functions of $\alpha$, $\alpha'$. If then $\alpha$ and $\alpha'$ are given as functions, say of $s$ and $s'$, this makes seven equations between

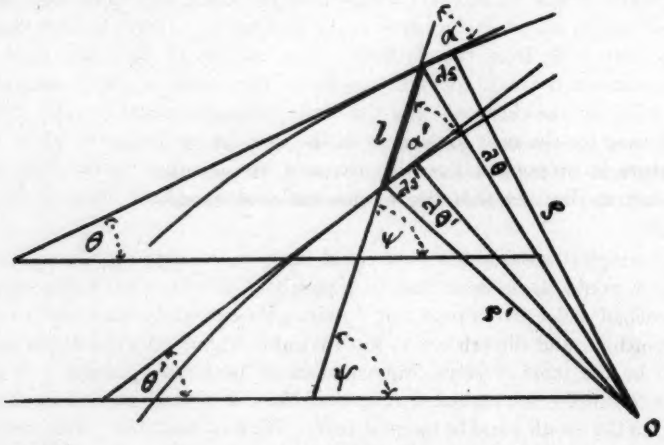


FIG. 2

the variables $\alpha$, $\alpha'$, $\theta$, $\theta'$, $s$, $s'$, $\rho$, $\rho'$, so that we may find the differential equations of the path of either the front or rear wheel. In particular, if $\alpha$ and $\alpha'$ are constant and equal, we shall have merely a movement of translation, while if $\alpha' = 0$, $\alpha =$ constant we shall describe two concentric circles. If $\alpha' = 0$, $\alpha = 90°$, the machine will describe a circle about the rear wheel. If, with these values of $\alpha$, $\alpha'$ the length $l$ be made variable, and a given function of $s$, the front wheel will describe a curve and the rear wheel its evolute. Thus a curve may be mechanically constructed from its intrinsic equation. This principle is used in certain integrating machines, and the author has invented an integrator for drawing trajectories involving this principle, which will be described later if he succeeds in having it built.

In the case of the automobile we have

$$\alpha' = 0, \qquad \rho = l\text{ctn}\alpha, \qquad ds = l\text{ctn}\alpha d\theta,$$

and if as before we assume the mode of steering to be $\alpha = as$ we may integrate and obtain the intrinsic equation of the curve,

$$ld\theta = \tan(as)ds, \qquad la\theta = \log \sec as.$$

Developing the tangent in series we may see how much this differs from the Cornu spiral. The curve has been drawn graphically from the differential equation, but since on a sixty-foot chord it differs but slightly from

the spiral (which may be judged from the fact that for $\theta = 45°$, $\alpha = 23°.2'$; $\rho = 22.35$ compared with $\rho = 22.28$ for the spiral, and that the rear wheel's track is less than two feet distant at the maximum) it is not here reproduced.

It may be said that the above is not applicable to the way in which an automobile actually skids, when it is well known that the two wheels do not break the frictional constraint together, but the rear wheel generally skids first. This may be true, but I think this will not invalidate anything that I have said. One would suppose that this question would be treated in any elementary book on statics, but as I have failed to find it in any treatise, I insert a treatment here. It will now be necessary to consider a third path, namely, that of the center of gravity of the machine, which we shall still assume to be on the line joining the wheels, at distances $d$ and $d'$ therefrom, figure 3. Then we have $d'\text{ctn}\alpha'' = (d + d')\text{ctn}\alpha$. The three

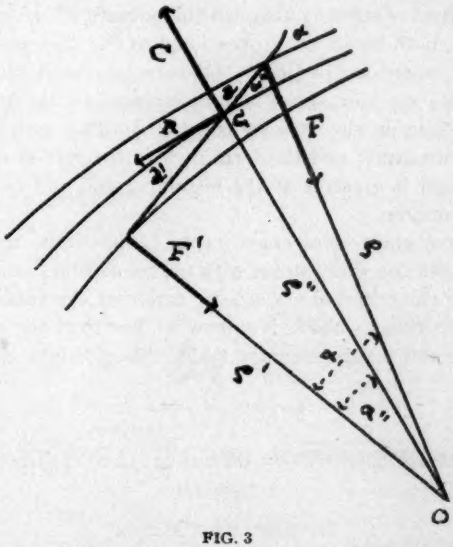


FIG. 3

paths have the same center of curvature. The constraints due to the friction can be only at right angles to the paths of the wheels, and we will call them $F$, $F'$. The kinetic reaction of the machine is described by the centrifugal force $C$, the tangential reaction $R$, and the moment $S$. It may be asked how the wheels can cause any reaction in the path, but it will be seen that there must be such when we consider that energy of translation being converted into energy of rotation and conversely will give rise to acceleration in the path, negative or positive, respectively. In fact we see at once that $S$ must vanish with $R$, for three concurrent

forces do not give rise to any moment. Resolving parallel and perpendicular to the chassis,

$$F' + F\cos\alpha = C\cos\alpha'' + R\sin\alpha'',$$
$$F\sin\alpha = C\sin\alpha'' - R\cos\alpha'',$$

and taking moments about the center of mass,

$$F'd' - Fd\cos\alpha = S,$$

or making use of the relation between $\alpha$ and $\alpha''$,

$$F' - F\sin(\alpha-\alpha'')/\sin\alpha'' = S/d'.$$

Solving these equations we obtain

$$R = -S/d'\sin\alpha'',$$
$$F = \sin\alpha''/\sin\alpha\ (C + S\cos\alpha''/d'),$$
$$F' = \sin(\alpha - \alpha'')/\sin\alpha\ C + S/d'\ (\sin(\alpha-\alpha'')\cos\alpha''/\sin\alpha - 1).$$

Now since $C = mv^2/\rho''$ and $S = mk^2d^2\psi/dt^2 = mk^2(d^2\theta/dt^2 + d^2\alpha''/dt^2)$ and in the method of steering assumed this is $mk^2d^2\theta''/dt^2 = mk^2v^2d^2\theta/ds^2$, if $v$ is constant, both terms are proportional to $v^2$. Consequently the conclusions above stated are justified. (It is to be remarked that if $v$ is constant, the kinetic reaction above is to be replaced by the force of traction necessary to maintain the velocity constant.) The term in $C$ is proportional to the curvature, and the term in $S$ to the rate of increase of curvature, the latter is greatest at the beginning and end of the curve, the former at the middle.

Finally I have made some experiments to determine the coefficient of friction $\mu$ of rubber on slimy stone, with the conclusion that it is about one-fourth. Using the criterion $v^2 < \mu g\rho$ we arrive at the conclusion that the safe speed for curves as above is somewhat less than ten miles per hour, which may account for the common traffic rule of "eight miles around the corner."

---

## *THE PROBABLE ERROR OF THE VITAL INDEX OF A POPULATION*[1]

BY JOHN RICE MINER

DEPARTMENT OF BIOMETRY AND VITAL STATISTICS, JOHNS HOPKINS UNIVERSITY

Communicated February 14, 1922

In comparing the birth-death ratios of different communities we need their probable errors to determine the significance of observed differences.

Let $N$ = the population of a community,
$B$ = number of births in a year,
$D$ = number of deaths in a year.

Then the birth-death ratio or vital index is defined as $\frac{100\,B}{D}$.

The standard errors of sampling of births and deaths will be:

$$\sigma_B = \sqrt{\frac{B(N-B)}{N}} \qquad \sigma_D = \sqrt{\frac{D(N-D)}{N}}$$

whence $V_B = \frac{\sigma_B}{B} = \sqrt{\frac{1-B/N}{B}}$ $\qquad V_D = \frac{\sigma_D}{D} = \sqrt{\frac{1-D/N}{D}}$

and the probable error of the birth-death ratio will be[2]

$$PE\left\{\frac{100\,B}{D}\right\} = 67.449\,\frac{B}{D}\sqrt{\frac{1-B/N}{B} + \frac{1-D/N}{D}} \qquad \text{(i)}$$

since $r = 0$, being the correlation of errors of sampling of births and deaths. As $B$ and $D$ are small as compared with $N$ we may write this approximately:

$$PE\left\{\frac{100\,B}{D}\right\} = 67.449\,\frac{B}{D}\sqrt{\frac{1}{B} + \frac{1}{D}} \qquad \text{(ii)}$$

This form has the advantage of not involving $N$, so that if the numbers of births and deaths in a community are known but not the population, the probable error of the birth-death ratio may still be found.

For Baltimore in 1917

$N = 594{,}637$
$B = 15{,}040$
$D = 11{,}355.$

Therefore by (i)

$$PE\left\{\frac{100\,B}{D}\right\} = 67.449\,\frac{15040}{11355}\sqrt{\frac{1-\frac{15040}{594637}}{15040} + \frac{1-\frac{11355}{594637}}{11355}}$$

$$= 89.34\sqrt{\frac{0.9747}{15040} + \frac{0.9809}{11355}} = 89.34\ \sqrt{.00006481 + .00008638}$$

$$= 89.34 \times .01229 = 1.10.$$

By (ii)

$$PE\left\{\frac{100\,B}{D}\right\} = 67.449\,\frac{15040}{11355}\ \sqrt{\frac{1}{15040} + \frac{1}{11355}} = 89.34\ \sqrt{.00006649 + .00008807}$$

$$= 89.34 \times .01243 = 1.11.$$

In using these formulae it should be borne in mind that the expression for the standard deviation of an index, which has been used in their derivation, is obtained on the assumption that deviations are small compared with the mean values of the variables. This will be true if $B$ and $D$ are of

fair size, but the formulae should not be used for very small absolute numbers of births and deaths.

[1] Papers from the Department of Biometry and Vital Statistics, School of Hygiene and Public Health, Johns Hopkins University, No. 52.

[2] Pearson, K. On a form of spurious correlation which may arise when indices are used in the measurement of organs. *Proc. Roy. Soc.*, **60**, 1897 (489).

---

## THE AVERAGE CHEMICAL COMPOSITION OF IGNEOUS ROCKS

BY FRANK W. CLARKE AND HENRY S. WASHINGTON

U. S. GEOLOGICAL SURVEY* AND GEOPHYSICAL LABORATORY OF THE CARNEGIE INSTITUTION OF WASHINGTON

Communicated March 22, 1922

We have recently completed computations of the average chemical composition of the igneous rocks of various countries, of the continents, and of the earth's crust. These are to be published as a *Professional Paper* of the U. S. Geological Survey, with discussions of the characters of the various averages, of the relative abundance, distribution, association, and evolution of the elements, and other matters. Inasmuch as it is probable that this paper will not appear for a considerable time, it is thought best to publish now the various average compositions arrived at, in order to put before geologists and others some interesting data as to the chemical composition of the earth.

The data used by us were 5,159 chemical analyses of igneous rocks from all over the earth, and published between 1884 and 1913, inclusive. Analyses only of "superior" quality, and of fresh unaltered rocks, were considered. These were taken from a collection of rock analyses made by one of us.[1] In computing the averages of the various countries and the continents the sum total of each constituent was divided by the total number of analyses of rocks from the area dealt with. In the case of the earth average, both in terms of oxides and of elements, the same method was adopted for the major constituents, $SiO_2$, $Al_2O_3$, $Fe_2O_3$, FeO, MgO, CaO, $Na_2O$, $K_2O$ and $H_2O$ (only water above 110° was considered), while the average for the minor constituents was obtained by taking the mean of the sum total of each divided by the number of analyses (which gives too low a result) and by the number of determinations (which is apt to give too high a result).

In computing the average of the whole crust the relative proportions estimated by one of us[2] some years ago were adopted. The latest estimates of the masses and compositions of the hydrosphere and atmosphere have been used. These relative masses are as follows: Lithosphere 93%; hydrosphere 7%; atmosphere 0.03%.

AVERAGE IGNEOUS ROCKS, UNITED STATES

| | 1 | 2 | 3 | 4 | 5 | 6 | 7 | 8 | 9 | 10 | 11 | 12 |
|---|---|---|---|---|---|---|---|---|---|---|---|---|
| $SiO_2$ | 61.41 | 62.98 | 57.81 | 58.54 | 60.37 | 60.03 | 60.09 | 65.80 | 61.39 | 59.97 | 62.49 | 60.77 |
| $Al_2O_3$ | 15.20 | 14.74 | 15.43 | 16.36 | 15.26 | 16.16 | 15.94 | 15.52 | 16.24 | 15.90 | 15.71 | 15.44 |
| $Fe_2O_3$ | 2.47 | 1.86 | 4.60 | 3.74 | 2.53 | 2.91 | 3.41 | 2.17 | 2.84 | 2.11 | 1.97 | 2.77 |
| FeO | 4.21 | 3.69 | 5.98 | 2.36 | 3.07 | 2.44 | 2.86 | 1.60 | 2.85 | 4.13 | 3.01 | 3.46 |
| MgO | 3.01 | 3.70 | 3.52 | 2.54 | 3.77 | 3.26 | 2.34 | 1.52 | 2.74 | 4.38 | 3.67 | 3.15 |
| CaO | 4.46 | 4.69 | 4.64 | 4.11 | 4.80 | 4.49 | 4.85 | 3.44 | 4.81 | 6.11 | 5.67 | 4.82 |
| $Na_2O$ | 3.94 | 3.30 | 3.60 | 5.35 | 3.82 | 4.08 | 3.86 | 3.49 | 4.18 | 3.71 | 3.57 | 3.78 |
| $K_2O$ | 3.30 | 2.97 | 2.31 | 4.68 | 3.99 | 3.81 | 3.90 | 4.10 | 3.04 | 1.55 | 2.03 | 3.23 |
| $H_2O^+$ | 0.74 | 0.82 | 0.98 | 1.04 | 1.03 | 1.49 | 1.12 | 1.40 | 0.69 | 1.11 | 1.05 | 1.01 |
| $TiO_2$ | 0.91 | 0.89 | 0.73 | 0.76 | 0.58 | 0.64 | 0.88 | 0.55 | 0.72 | 0.66 | 0.45 | 1.01 |
| $ZrO_2$ | 0.01 | 0.01 | 0.00 | 0.03 | .... | .... | 0.01 | 0.01 | .... | .... | .... | .... |
| $P_2O_5$ | 0.11 | 0.20 | 0.08 | 0.19 | 0.32 | 0.30 | 0.34 | 0.13 | 0.31 | 0.17 | 0.15 | 0.29 |
| MnO | 0.09 | 0.08 | 0.16 | 0.10 | 0.10 | 0.06 | 0.12 | 0.04 | 0.11 | 0.06 | 0.09 | 0.10 |
| BaO | 0.01 | 0.01 | 0.01 | 0.02 | 0.15 | 0.08 | 0.07 | 0.05 | 0.04 | 0.05 | 0.05 | 0.05 |
| Incl. | 0.13 | 0.06 | 0.15 | 0.18 | 0.21 | 0.25 | 0.21 | 0.18 | 0.05 | 0.07 | 0.09 | 0.12 |
| | 100.00 | 100.00 | 100.00 | 100.00 | 100.00 | 100.00 | 100.00 | 100.00 | 100.00 | 100.00 | 100.00 | 100.00 |

1. New England and New York. 213 analyses.
2. Appalachia (New Jersey and Pennsylvania to Georgia). 188 analyses.
3. Algonkian Region (Michigan, Wisconsin, and Minnesota). 66 analyses.
4. Arkansas-Texas, including Missouri. 50 analyses.
5. Wyoming, including South Dakota and Yellowstone Park. 134 analyses.
6. Montana, including Idaho. 133 analyses.
7. Colorado. 171 analyses.
8. Utah and Nevada. 79 analyses.
9. Arizona and New Mexico. 79 analyses.
10. Washington and Oregon. 51 analyses.
11. California. 175 analyses.
12. United States. 1351 analyses, including analyses of 12 highly femic and titaniferous rocks omitted from the other columns.

AVERAGE IGNEOUS ROCKS, EUROPE

| | 1 | 2 | 3 | 4 | 5 | 6 | 7 | 8 | 9 | 10 | 11 | 12 | 13 |
|---|---|---|---|---|---|---|---|---|---|---|---|---|---|
| $SiO_2$ | 59.84 | 59.10 | 62.39 | 56.89 | 59.83 | 64.04 | 60.59 | 58.83 | 56.93 | 60.69 | 58.98 | 54.22 | 64.73 |
| $Al_2O_3$ | 15.12 | 13.80 | 15.16 | 15.54 | 16.08 | 14.24 | 16.43 | 14.44 | 15.86 | 14.67 | 16.28 | 16.30 | 15.92 |
| $Fe_2O_3$ | 3.17 | 3.14 | 2.40 | 2.69 | 3.65 | 3.65 | 2.75 | 3.35 | 3.72 | 2.76 | 2.53 | 4.28 | 3.15 |
| FeO | 3.67 | 4.57 | 3.04 | 3.57 | 3.21 | 3.41 | 2.88 | 3.91 | 3.78 | 3.28 | 3.44 | 5.54 | 2.28 |
| MgO | 3.61 | 4.80 | 3.79 | 4.57 | 2.26 | 1.82 | 2.16 | 4.63 | 4.15 | 4.56 | 3.03 | 5.02 | 1.76 |
| CaO | 4.97 | 5.41 | 3.92 | 4.43 | 3.64 | 3.25 | 3.35 | 5.56 | 6.45 | 4.37 | 5.16 | 7.60 | 4.49 |
| $Na_2O$ | 3.73 | 3.55 | 3.70 | 4.56 | 5.10 | 3.70 | 6.11 | 3.45 | 3.61 | 3.52 | 3.72 | 2.99 | 3.69 |
| $K_2O$ | 3.40 | 2.68 | 3.23 | 4.47 | 3.52 | 3.82 | 3.96 | 3.04 | 2.96 | 3.56 | 4.67 | 1.92 | 2.56 |
| $H_2O^+$ | 1.24 | 1.44 | 1.46 | 1.19 | 0.75 | 0.84 | 0.71 | 1.40 | 1.45 | 1.68 | 0.94 | 1.17 | 1.03 |
| $TiO_2$ | 0.83 | 0.97 | 0.75 | 1.34 | 1.64 | 0.73 | 0.56 | 0.87 | 0.58 | 0.65 | 0.85 | 0.66 | 0.31 |
| $P_2O_5$ | 0.23 | 0.22 | 0.12 | 0.34 | 0.12 | 0.25 | 0.27 | 0.29 | 0.27 | 0.19 | 0.22 | 0.07 | 0.03 |
| MnO | 0.08 | 0.14 | 0.01 | 0.07 | 0.10 | 0.15 | 0.19 | 0.04 | 0.14 | 0.03 | 0.04 | 0.14 | 0.03 |
| Incl. | 0.11 | 0.18 | 0.03 | 0.34 | 0.10 | 0.10 | 0.05 | 0.18 | 0.10 | 0.04 | 0.14 | 0.09 | 0.02 |
| | 100.00 | 100.00 | 100.00 | 100.00 | 100.00 | 100.00 | 100.00 | 100.00 | 100.00 | 100.00 | 100.00 | 100.00 | 100.00 |

1. Europe. 1985 analyses.
2. British Islands. 171 analyses.
3. France, including Corsica. 163 analyses.
4. Iberia (Spain and Portugal). 33 analyses.
5. Norway, including Iceland. 107 analyses.
6. Sweden, including Spitzbergen. 206 analyses.
7. Finland, including Kola. 59 analyses.
8. Germany. 474 analyses.
9. Austria-Hungary-Bohemia, excluding Tyrol. 148 analyses.
10. Switzerland, including Tyrol. 217 analyses.
11. Italy, including Sicily, Sardinia, and islands. 276 analyses.
12. Russia, including Urals and Caucasus, excluding Finland and Siberia. 98 analyses.
13. Balkania, including Greece and Archipelago. 33 analyses.

AVERAGE IGNEOUS ROCKS, AFRICA AND ASIA

| | 1 | 2 | 3 | 4 | 5 | 6 | 7 | 8 |
|---|---|---|---|---|---|---|---|---|
| $SiO_2$ | 58.21 | 54.67 | 50.59 | 56.02 | 61.92 | 61.81 | 59.72 | 61.02 |
| $Al_2O_3$ | 15.28 | 16.21 | 15.81 | 15.68 | 15.49 | 15.73 | 16.51 | 15.97 |
| $Fe_2O_3$ | 3.52 | 3.02 | 4.44 | 3.48 | 3.17 | 2.07 | 3.18 | 2.92 |
| FeO | 3.73 | 4.93 | 5.79 | 4.41 | 2.75 | 4.41 | 2.95 | 3.21 |
| MgO | 3.51 | 4.21 | 5.79 | 4.04 | 2.63 | 2.47 | 3.03 | 2.76 |
| CaO | 5.09 | 6.51 | 7.36 | 5.87 | 4.50 | 5.16 | 5.76 | 5.17 |
| $Na_2O$ | 4.83 | 4.36 | 4.27 | 4.60 | 4.10 | 3.11 | 3.78 | 3.69 |
| $K_2O$ | 3.28 | 3.05 | 2.31 | 3.07 | 3.23 | 2.51 | 3.05 | 2.99 |
| $H_2O^+$ | 1.26 | 1.13 | 1.47 | 1.25 | 1.23 | 1.48 | 1.11 | 1.24 |
| $TiO_2$ | 0.84 | 1.44 | 1.63 | 1.14 | 0.68 | 0.76 | 0.50 | 0.62 |
| $P_2O_5$ | 0.20 | 0.35 | 0.43 | 0.27 | 0.12 | 0.27 | 0.18 | 0.18 |
| MnO | 0.07 | 0.01 | 0.04 | 0.05 | 0.10 | 0.17 | 0.14 | 0.15 |
| BaO | .... | .... | .... | .... | .... | .... | .... | .... |
| Incl. | 0.18 | 0.11 | 0.07 | 0.12 | 0.08 | 0.03 | 0.09 | 0.08 |
| | 100.00 | 100.00 | 100.00 | 100.00 | 100.00 | 100.00 | 100.00 | 100.00 |

1. Africa, continental. 223 analyses.
2. Madagascar, including Reunion. 140 analyses.
3. South Atlantic Islands (Azores, Canaries, Madeira, Cape Verde, Ascension, St. Helena). 56 analyses.
4. Africa and islands, including Madagascar and Atlantic Islands. 419 analyses.
5. Asia, continental. 114 analyses.
6. Japan. 69 analyses.
7. Malaysia, including Philippines. 129 analyses.
8. Asia, including continent, Malaysia and Japan. 312 analyses.

AVERAGE IGNEOUS ROCKS, AUSTRALASIA, POLYNESIA, ANTARCTICA

| | 1 | 2 | 3 | 4 |
|---|---|---|---|---|
| $SiO_2$ | 60.16 | 58.04 | 50.03 | 53.66 |
| $Al_2O_3$ | 14.74 | 15.30 | 15.51 | 16.82 |
| $Fe_2O_3$ | 2.60 | 3.83 | 3.88 | 4.01 |
| FeO | 4.41 | 3.99 | 6.23 | 5.34 |
| MgO | 3.76 | 3.95 | 6.62 | 4.67 |
| CaO | 5.03 | 5.39 | 7.99 | 7.59 |
| $Na_2O$ | 3.50 | 3.78 | 4.00 | 3.58 |
| $K_2O$ | 3.03 | 2.93 | 2.10 | 2.32 |
| $H_2O^+$ | 1.19 | 1.70 | 1.16 | 0.93 |
| $TiO_2$ | 1.01 | 0.71 | 1.96 | 0.87 |
| $P_2O_5$ | 0.26 | 0.19 | 0.25 | 0.17 |
| MnO | 0.15 | 0.09 | 0.15 | 0.03 |
| BaO | 0.02 | .... | .... | .... |
| Incl. | 0.14 | 0.10 | 0.12 | 0.01 |
| | 100.00 | 100.00 | 100.00 | 100.00 |

1. Australia, including Tasmania. 287 analyses.
2. New Zealand, including dependent islands. 134 analyses.
3. Polynesia (Hawaiian Islands, etc.). 72 analyses.
4. Antarctica and adjacent islands. 103 analyses.

**AVERAGE CHEMICAL COMPOSITION OF THE IGNEOUS ROCKS OF THE EARTH**

| | |
|---|---|
| $SiO_2$ | 59.12 |
| $Al_2O_3$ | 15.34 |
| $Fe_2O_3$ | 3.08 |
| FeO | 3.80 |
| MgO | 3.49 |
| CaO | 5.08 |
| $Na_2O$ | 3.84 |
| $K_2O$ | 3.13 |
| $H_2O^+$ | 1.15 |
| $CO_2$ | 0.101 |
| $TiO_2$ | 1.050 |
| $ZrO_2$ | 0.039 |
| $P_2O_5$ | 0.299 |
| Cl | 0.048 |
| F | 0.030 |
| S | 0.052 |
| $(Ce,Y)_2O_3$ | 0.020 |
| $Cr_2O_3$ | 0.055 |
| $V_2O_3$ | 0.026 |
| MnO | 0.124 |
| NiO | 0.025 |
| BaO | 0.055 |
| SrO | 0.022 |
| $Li_2O$ | 0.008 |
| Cu | 0.010 |
| Zn | 0.004 |
| Pb | 0.002 |
| | 100.000 |

**AVERAGE COMPOSITION OF IGNEOUS ROCKS IN TERMS OF ELEMENTS**

| | | 1 | 2 | 3 |
|---|---|---|---|---|
| 1 | Oxygen | 46.41 | 47.29 | 47.2 |
| 2 | Silicon | 27.58 | 28.02 | 28.0 |
| 3 | Aluminum | 8.08 | 7.96 | 8.0 |
| 4 | Iron | 5.08 | 4.56 | 4.5 |
| 5 | Calcium | 3.61 | 3.47 | 3.5 |
| 6 | Sodium | 2.83 | 2.50 | 2.5 |
| 7 | Potassium | 2.58 | 2.47 | 2.5 |
| 8 | Magnesium | 2.09 | 2.29 | 2.5 |
| 9 | Titanium | 0.720 | 0.46 | 0.33 |
| 10 | Phosphorus | 0.157 | 0.13 | 0.22 |
| 11 | Hydrogen | 0.129 | 0.16 | 0.17 |
| 12 | Manganese | 0.124 | 0.078 | 0.075 |
| 13 | Chlorine | 0.096 | 0.063 | 0.04–.025 |
| 14 | Barium | 0.081 | 0.093 | 0.03 |
| 15 | Sulphur | 0.080 | 0.10 | 0.06 |
| 16 | Chromium | 0.068 | 0.034 | 0.01 |
| 17 | Zirconium | 0.052 | 0.017 | 0.02–.01 |
| 18 | Carbon | 0.051 | 0.13 | 0.22 |
| 19 | Vanadium | 0.041 | 0.017 | 0.00x |
| 20 | Strontium | 0.034 | 0.034 | 0.005 |
| 21 | Nickel | 0.031 | 0.020 | 0.005 |
| 22 | Fluorine | 0.030 | 0.10 | 0.04–.025 |
| 23 | Cerium, Yttrium | 0.020 | ..... | 0.00x,x |
| 24 | Copper | 0.010 | ..... | 0.000,xx |
| 25 | Lithium | 0.005 | 0.004 | 0.004 |
| 26 | Zinc | 0.004 | ..... | 0.000,x |
| 27 | Cobalt | 0.003 | ..... | 0.00x,x |
| 28 | Lead | 0.002 | ..... | 0.000,x |
| 29 | Boron | 0.001 | ..... | 0.00x |
| 30 | Glucinum | 0.001 | ..... | 0.00x |
| | | 100.000 | 100.000 | 100.000 |

1. Igneous rocks. Clarke and Washington, 1922.
2. Igneous rocks. Clarke, *Bull.* **695**, 1920, p. 28.
3. Igneous rocks. Vogt, *Zeits. praki. Geol.*, **1898**, p. 324.

AVERAGE IGNEOUS ROCKS, NORTHERN NORTH AMERICA

| | 1 | 2 | 3 | 4 | 5 | 6 |
|---|---|---|---|---|---|---|
| $SiO_2$ | 60.19 | 57.14 | 63.31 | 56.19 | 52.70 | 58.34 |
| $Al_2O_3$ | 15.76 | 15.48 | 16.67 | 16.67 | 16.38 | 15.79 |
| $Fe_2O_3$ | 2.87 | 3.93 | 2.18 | 3.31 | 4.58 | 2.21 |
| FeO | 3.67 | 4.72 | 2.46 | 4.65 | 5.83 | 3.99 |
| MgO | 3.16 | 1.55 | 2.25 | 3.39 | 3.27 | 4.57 |
| CaO | 4.80 | 3.51 | 5.05 | 5.34 | 5.29 | 5.66 |
| $Na_2O$ | 3.90 | 6.98 | 3.85 | 4.40 | 4.88 | 3.54 |
| $K_2O$ | 3.07 | 3.25 | 2.82 | 3.00 | 2.65 | 3.18 |
| $H_2O^+$ | 1.01 | 1.12 | 0.78 | 1.08 | 1.09 | 1.14 |
| $TiO_2$ | 1.01 | 1.50 | 0.77 | 1.25 | 2.20 | 0.69 |
| $ZrO_2$ | 0.01 | 0.12 | .... | .... | .... | .... |
| $P_2O_5$ | 0.26 | 0.19 | 0.18 | 0.19 | 0.21 | 0.33 |
| MnO | 0.10 | 0.21 | 0.10 | 0.13 | 0.17 | 0.14 |
| BaO | 0.04 | .... | .... | 0.04 | 0.06 | 0.11 |
| Incl. | 0.15 | 0.30 | 0.12 | 0.26 | 0.59 | 0.31 |
| | 100.00 | 100.00 | 100.00 | 100.00 | 100.00 | 100.00 |

1. North America, including Greenland, Mexico, Central America, and West Indies 1709 analyses.
2. Greenland, including East and West Greenland and Ellesmere Land. 41 analyses.
3. Alaska. 24 analyses.
4. Canada, including Alaska, East Canada, and British Columbia. 188 analyses.
5. East Canada, including Ontario, Quebec, Maritime Provinces, and Newfoundland. 99 analyses.
6. British Columbia, including Alberta. 60 analyses.

AVERAGE IGNEOUS ROCKS, MIDDLE AND SOUTH AMERICA

| | 1 | 2 | 3 | 4 | 5 | 6 |
|---|---|---|---|---|---|---|
| $SiO_2$ | 59.11 | 58.70 | 61.34 | 61.06 | 61.85 | 54.92 |
| $Al_2O_3$ | 16.58 | 18.30 | 15.20 | 15.17 | 16.51 | 16.29 |
| $Fe_2O_3$ | 2.88 | 2.85 | 3.03 | 2.42 | 3.03 | 4.05 |
| FeO | 4.11 | 4.20 | 3.30 | 4.07 | 2.28 | 3.53 |
| MgO | 3.07 | 3.36 | 3.47 | 4.65 | 2.29 | 4.33 |
| CaO | 5.73 | 7.08 | 4.88 | 5.91 | 4.55 | 5.28 |
| $Na_2O$ | 4.10 | 3.15 | 4.09 | 3.29 | 4.47 | 5.11 |
| $K_2O$ | 2.32 | 0.99 | 2.69 | 1.74 | 2.69 | 3.57 |
| $H_2O$ | 1.04 | 0.79 | 1.05 | 0.73 | 1.11 | 1.55 |
| $TiO_2$ | 0.63 | 0.45 | 0.56 | 0.49 | 0.75 | 0.87 |
| $P_2O_5$ | 0.25 | 0.08 | 0.11 | 0.07 | 0.25 | 0.11 |
| MnO | 0.06 | 0.02 | 0.12 | 0.18 | 0.22 | 0.37 |
| Incl. | 0.12 | 0.03 | 0.16 | 0.13 | .... | .... |
| | 100.00 | 100.00 | 100.00 | 100.00 | 100.00 | 100.00 |

1. Mexico and Central America. 47 analyses.
2. West Indies. 82 analyses.
3. South America. 138 analyses.
4. British Guiana. 45 analyses.
5. Andes Mountains. 56 analyses.
6. Eastern Brazil (including Paraguay and eastern Argentina). 20 analyses.

RARER ELEMENTS IN IGNEOUS ROCKS

| | 1 | 2 |
|---|---|---|
| Rubidium | .000,x | .00x,x |
| Arsenic | .000,x | .00x,x |
| Molybdenum | .000,x | .000,0x |
| Tin | .000,x | .00x,x |
| Bromine | .000,x | .00x |
| Caesium | .000,0x | .000,00x |
| Scandium | .000,0x | .000,000,000,xx |
| Antimony | .000,0x | .00x,x |
| Cadmium | .000,0x | .000,00x |
| Mercury | .000,0x | .000,00x |

RARER ELEMENTS IN IGNEOUS ROCKS (*Continued*)

| | 1 | 2 |
|---|---|---|
| Iodine | .000,0x | .00x,x |
| Bismuth | .000,00x | .000,000,x |
| Tungsten | .000,00x | .000,00x |
| Thorium | .000,00x | .000,000,x |
| Columbium, Tantalum | .000,00x | .000,000,x |
| Uranium | .000,00x | .000,00x |
| Silver | .000,00x | .000,00o,x |
| Selenium | .000,00x | .000,000,x |
| Platinum | .000,000,x | .000,000,0x |
| Tellurium | .000,000,x | .000,000,0x |
| Gold | .000,000,x | .000,000,0x |
| Thallium | .000,000,0x | .000,000,00x |
| Indium | .000,000,00x | .000,000,00x |
| Gallium | .000,000,00x | .000,000,00x |
| Germanium | .000,000,000,x | .000,000,000,x |
| Radium | .000,000,000,00x | ..... |

1. Clarke and Washington, 1922.
2. Vogt, 1898.

ELEMENTS IN THE LITHOSPHERE, HYDROSPHERE, AND ATMOSPHERE

| | 1 | 2 | 3 | 4 |
|---|---|---|---|---|
| Oxygen | 49.19 | 47.80 | 46.68 | 46.41 |
| Silicon | 25.71 | 26.65 | 27.60 | 27.58 |
| Aluminum | 7.50 | 7.79 | 8.05 | 8.08 |
| Iron | 4.68 | 4.88 | 5.03 | 5.08 |
| Calcium | 3.37 | 3.49 | 3.63 | 3.61 |
| Sodium | 2.61 | 2.72 | 2.72 | 2.83 |
| Potassium | 2.38 | 2.48 | 2.56 | 2.58 |
| Magnesium | 1.94 | 2.01 | 2.07 | 2.09 |
| Hydrogen | 0.872 | 0.497 | 0.145 | 0.129 |
| Titanium | 0.648 | 0.684 | 0.696 | 0.720 |
| Chlorine | 0.228 | 0.162 | 0.095 | 0.096 |
| Phosphorus | 0.142 | 0.150 | 0.152 | 0.157 |
| Carbon | 0.139 | 0.095 | 0.149 | 0.051 |
| Manganese | 0.108 | 0.116 | 0.116 | 0.124 |
| Sulphur | 0.093 | 0.086 | 0.100 | 0.080 |
| Barium | 0.075 | 0.078 | 0.079 | 0.081 |
| Chromium | 0.062 | 0.065 | 0.066 | 0.068 |
| Zirconium | 0.048 | 0.050 | 0.052 | 0.052 |
| Vanadium | 0.038 | 0.040 | 0.041 | 0.041 |
| Strontium | 0.032 | 0.034 | 0.034 | 0.034 |
| Fluorine | 0.030 | 0.030 | 0.030 | 0.030 |
| Nickel | 0.030 | 0.031 | 0.031 | 0.031 |
| Nitrogen | 0.030 | 0.016 | .... | .... |
| Cerium, Yttrium | 0.019 | 0.020 | 0.020 | 0.020 |
| Copper | 0.010 | 0.010 | 0.010 | 0.010 |
| Lithium | 0.005 | 0.005 | 0.005 | 0.005 |
| Zinc | 0.004 | 0.004 | 0.004 | 0.004 |
| Cobalt | 0.003 | 0.003 | 0.003 | 0.003 |
| Lead | 0.002 | 0.002 | 0.002 | 0.002 |
| Boron | 0.001 | 0.001 | 0.001 | 0.001 |
| Glucinum | 0.001 | 0.001 | 0.001 | 0.001 |
| | 100.000 | 100.000 | 100.000 | 100.000 |

1. Average composition. Ten-mile crust, hydrosphere, and atmosphere.
2. Average composition. Twenty-mile crust, hydrosphere, atmosphere.
3. Average composition. Ten-mile crust, igneous and sedimentary rocks.
4. Average composition. Ten-mile crust. Igneous rocks.

The lithosphere is assumed to be made up as follows: Igneous rocks 95.00%; shale 4.00%; sandstone 0.75%; limestone 0.25%.

In the calculations involving the atmosphere and hydrosphere the thickness of the crust is assumed to be ten (or twenty) miles.

* Published with the permission of the Director of the U. S. Geological Survey.

[1] H. S. Washington, "Chemical Analyses of Igneous Rocks," *U. S. Geol. Survey, Prof. Paper* 99 (1917).

[2] F. W. Clarke, "The Data of Geochemistry," *U. S. Geol. Survey, Bull.* 695, 1920 (22 and 33).

---

## *DARK NEBULAE*

BY HENRY NORRIS RUSSELL

RESEARCH ASSOCIATE, MOUNT WILSON OBSERVATORY, CARNEGIE INSTITUTION OF WASHINGTON

Communicated March 14, 1922

1. It is now generally believed that many of the dark markings in the Milky Way, and dark starless regions in the sky, are produced by the interposition of huge obscuring clouds between us and the remoter stars. A long list of such dark markings has been given by Barnard,[1] who has done more than any one else to point out their importance and probable nature. In some cases, as in the Pleiades, Orion and Ophiuchus, these "regions of obscuration" merge into faintly luminous nebulosity in the vicinity of certain stars, in such a way that there can be no doubt that they lie near these stars in space.

It thus appears that the obscuring masses or dark nebulae in Ophiuchus and Scorpius are at a distance of from 100 to 150 parsecs, those in Taurus at probably about the same distance, and those in Orion some 200 parsecs from us, while the dimensions of the individual clouds are themselves measured in parsecs.

The occurrence of these three great regions of obscuration within a distance which is so small compared with that of the galactic clouds indicates that such objects are probably of great cosmical temperature.

2. These dark nebulae usually appear to be quite opaque. In some cases the stars can be seen faintly through them, apparently without much change in color; but in certain instances[2] stars imbedded in dense luminous nebulosity are abnormally red.

Of the various forms in which matter may be distributed in space, by far the most efficient in producing obscuration is fine dust, since this has the greatest superficial area per unit of mass. In a cloud composed of spherical particles of radius $r$ and density $\rho$, distributed at random so that the average quantity of matter per unit volume is $d$, the extinction of a beam of light in passing through this cloud will be $e$ stellar magnitudes per unit of distance, where $e = 0.814\ qd/\rho r$.

The numerical factor is independent of the physical units which are employed. The factor $q$ is introduced to take account of the complications which occur when the size of the particle becomes comparable with the wave-lengths of light.[3] For particles more than two or three wave-lengths in diameter $q$ is sensibly equal to unity. For smaller particles it increases and is a maximum, 2.56, when the circumference of the particle is 1.12 times the wave-length. It then rapidly diminishes and becomes nearly equal to $14/3 \times (2\pi r/\lambda)^4$ for particles of less than half this diameter. The ratio $q/r$ is a maximum, 2.42, when the circumference equals the wave-length.

For clouds of the same mean density $d$ the opacity reaches a sharp maximum when the particles are of this size. At the same time the absorption changes from the non-selective type to the selective type, varying as $\lambda^{-4}$. For visual light the maximum opacity occurs when the radius is $0.086\ \rho$. A cloud of particles of this size, and of the density of rock (2.7), will exert an absorption of one magnitude if it contains only 1/86 of a milligram of matter per square centimeter of cross-section, regardless of its thickness. If the particles are of half this size, or smaller, the selective absorption is almost as complete as for a gas, but may be nearly 100 million times as great.

Obscuration of light in space, therefore, whether general or selective with respect to wave-length, will be produced mainly by dust particles a few millionths of an inch in diameter, unless such particles form a negligible proportion by weight of the obscuring cloud.

3. It is just these particles, however, which will be most influenced by the pressure of the radiation of the stars. Calculations from more accurate data confirm Schwarzchild's conclusion that for a particle of the optimum size and the density of water, the repulsive force of the sun's radiation is about ten times the gravitational attraction, and show that for stars of the same brightness, but other spectral types, the radiation pressure will be about two-thirds as great for Class M and increase for the whiter stars, till for Class B it is fully ten times as great as for solar stars.

Dwarf stars will hardly repel dust at all, but giant stars, and especially the very luminous one of Class B, will repel it very powerfully. Only the coarser particles can come near such a star—the finer ones being driven away. This selective removal, from the vicinity of bright stars, of the particles which are most efficient in cloud formation, may explain the fact that the luminous portions of these dark nebulae, though centered upon stars, do not brighten up in their immediate neighborhood as much as might have been anticipated.

The finest dust must continue to be repelled by the stars, whatever their distance. It may congregate to some degree in interstellar regions,

where the repulsive forces from stars on opposite sides are nearly equal, but it can be in no true equilibrium there, and must ultimately escape to an indefinitely great distance.

4. Some force, however, operates to hold these dark clouds together, for their outlines are often sharp. This is probably the gravitational attraction of the cloud itself.

Taking a spherical cloud as an example we find that, if its mass is $M$ times that of the sun, and its radius $R$ parsecs, the velocity of escape at the surface is $0.092M^{\frac{1}{2}}R^{-\frac{1}{2}}$km./sec. The internal velocity of the nebular material is known only in the case of the Orion nebula, where the luminous gas shows irregular variations in radial velocity from point to point, amounting to about 5 km./sec.[5] on each side of the mean.

For a nebula 1 parsec in diameter (which may be taken as a rough representation of the small black, almost round spot about 15′ in diameter, discovered by Barnard[6] in Ophiuchus) the mass must be 60 times that of the sun, if the escape velocity is to be 1 km./sec.

If all this matter were in the form of particles of rock of the optimum size, the extinction for light passing centrally through the cloud would be 2000 magnitudes. An extinction of 10 magnitudes (quite sufficient for opacity) would be produced if the radius of the particles were 72 $\mu$.

Though these numerical values are largely conjectural, it appears probable that the aggregate mass contained in one of these great obscuring clouds must be very considerable—probably sufficient to form hundreds of stars—and that a sensible fraction of the whole mass must be in the form of dust less than 0.1 mm. in diameter.

It can easily be shown that any dust cloud which is impervious to light must also be impervious to particles such as those of which it is composed (and to free-moving electrons as well) in the sense that such a particle could not traverse the cloud without a practical certainty of collision. These collisions may account for the existence of dust within the clouds, even if it was not a primitive constituent.

5. The transition from these dark nebulae to luminous nebulae in the vicinity of the stars appears to occur in two ways. The first is by simple reflection of the light of the stars—which appears to occur in the nebulosity surrounding the Pleiades, the star $\rho$ Ophiuchi, and probably in many other cases. The second is by the excitation of gaseous emission, as in the Great Nebula of Orion, which is connected with one of the greatest known regions of obscuration and itself shows signs that obscuring masses lie in front of it.

Both theoretical considerations, as suggested by the writer[6] and the facts of observation collected by Hubble,[7] indicate that the luminosity of gaseous nebulae is probably due to excitation of the individual atoms by radiations of some sort (ethereal or corpuscular) emanating from neigh-

boring stars of very high temperature. In the Orion nebula the stars of the Trapezium ($\theta$ Orionis) appear to be the source of excitation.

There is no reason to believe that the luminous gas forms the whole, or even any large part, of the matter present within the region—only that it is selectively sensitive to the incident excitation, and therefore gives out most of the light, just as the gases (carbon compounds and nitrogen) do in the coma and tail of a comet.

If the turbulent motions of the various parts of this nebula are of the same order of magnitude in the other two coördinates as in the radial direction, they must correspond to an average proper motion of 1.5 astronomical units per year, or about $0''.8$ per century (with Kapteyn's parallax of $0''.0055$). In a million years this would carry a nebulous wisp through $2°$, which is more than the whole extent of the nebula.

It appears probable, therefore, that the aspect of the Orion nebula was entirely different a million years ago from what it is now, as regards its details. There is no reason, however, to suppose that the nebula was not there. We may rather imagine that wisps and clouds of dust, carrying gas with them, are slowly drifting about. Some of them pass through the field of excitation due to the radiations from the Trapezium stars, and, when in this field, the gas is set shining—faintly near its outskirts, and without excitation of the nebular lines; more strongly, and with the nebular lines, near the middle.

According to unpublished investigations by Hubble, it appears probable that the absorbing clouds in Orion, not far from the nebula, weaken the light of stars behind them by at least ten magnitudes. The exciting radiations probably penetrate to a relatively small depth into the mass and, even if they went deeper, little of the excited light could get out again. The Orion nebula, on this hypothesis, may be regarded almost as a superficial fluorescence of the gaseous portion of this vast dark cloud, in the limited region where it is stimulated by the influence of the exciting stars.

[1] Barnard, E. E., *Astrophys. J., Chicago*, **49**, 1919 (1–23).

[2] Seares, F. H., and E. P. Hubble, *Ibid.*, **52**, 1920 (8–22); *Mt. Wilson Contr.*, No. 187.

[3] Schwarzschild, K., *Sitzungsberichte der K. B. Akad. der Wiss., Math. Phys. Kl., München*, **31**, 1901 (293–338); Proudman, *Monthly Not., R. A. S., London*, **73**, 1913 (535–539).

[4] Barnard, E. E., *Astrophys. J., Chicago*, **38**, 1913 (496–501).

[5] *Publications of the Lick Observatory, Berkeley, Cal.*, **13**, 1918 (98).

[6] Russell, H. N., *The Observatory, London*, **44**, 1921 (72).

[7] Hubble, E. P., "Annual Report of the Mount Wilson Observatory," 1921; *Year Book of the Carnegie Institution of Washington*, **1921**.